JOURNAL OF CATALYSIS 133, 191–201 (1992)

Characterization of Zeolite-Supported Pt–Cu Bimetallic Catalyst by Xenon-129 NMR and EXAFS

D. H. AHN,* J. S. LEE,† M. NOMURA,‡ W. M. H. SACHTLER,§ G. MORETTI,§,[1] S. I. WOO,* AND R. RYOO‖,[2]

‖*Department of Chemistry, Korea Advanced Institute of Science and Technology, Taeduk Science Town, Taejon, 305-701 Korea; *Department of Chemical Engineering, Korea Advanced Institute of Science and Technology, P.O. Box 150, Cheongryang, Seoul, Korea; †Department of Chemical Engineering, Pohang Institute of Science and Technology, P.O. Box 125, Pohang, 680 Korea; ‡Photon Factory, National Laboratory for High Energy Physics, Tsukuba, Ibaraki 305, Japan; and §Department of Chemistry, Northwestern University, Evanston, Illinois 60208*

Received April 9, 1991; revised July 17, 1991

Samples of platinum supported on NaY zeolite (Pt/NaY), Cu/NaY, and bimetallic Pt–Cu/NaY have been prepared by using a scheme that consists of ion exchange of the metalammine cations, activation in flowing O_2, and subsequent reduction in H_2. These samples have been characterized by ^{129}Xe NMR and extended X-ray absorption fine structure (EXAFS). The chemical shift in ^{129}Xe NMR of the xenon adsorbed on Pt–Cu/NaY has been found to be significantly lower than that on Pt/NaY with the same Pt content under the same experimental conditions, and therefore bimetallic Pt–Cu clusters are formed in supercages of NaY zeolite in both the cases of a sequential clustering method and a simultaneous ion exchange preparation method. The peak intensities at Pt–Pt coordination distance in the Fourier transforms of EXAFS spectra for Pt/NaY and Pt–Cu/NaY are very similar, which indicates that the reduction of Cu precursor has resulted in no appreciable changes in the Pt–Pt coordination structure of the Pt cluster. It thus appears, from these results, that during the reduction of Cu precursor the bimetallic Pt–Cu clusters are formed with a model of a Cu covering on Pt clusters in the supercage of NaY zeolite.

INTRODUCTION

In a previous work with supported bimetallic catalysts, it was shown by one of the present authors that formation of alloy particles during catalyst reduction is strongly favored if the precursor of the less reducible metal is mobile over the surface of the support (*1–4*). For instance, if platinum is the easily reducible component of a bimetallic catalyst, its precursor will be reduced first, and the subsequent reduction of the other element is catalyzed by the platinum. The prevailing mechanism for this process includes surface migration of the mobile precursor: whenever it contacts a Pt particle in a reducing atmosphere, it will be reduced at a temperature that is often markedly lower than that required for its reduction in the absence of platinum. If alloy formation is thermodynamically possible, alloy particles are formed as a direct consequence of this catalyzed reduction mechanism. A hypothetical alternative mechanism, viz., hydrogen spillover from the reduced Pt particle via the support to the precursor of the second metal, is highly unlikely for supports on which chemisorption of hydrogen atom is energetically unfavorable and has indeed been ruled out experimentally for the catalyst system of Pt–Re/Al_2O_3 (*5*).

On amorphous supports, the precursors of the reduced metals are often oxides; in zeolites, however, metal precursors are often cations. Previous results obtained with the Pt–Cu/NaY bimetallic system are in conformity with the catalyzed reduction model: first Pt particles are formed in su-

[1] Present address: Department of Chemistry, University of "La Sapienza," Rome, Italy.

[2] To whom correspondence should be addressed.

0021-9517/92 $3.00

percages, and then mobile Cu^{2+} ions are adsorbed by these Pt particles and swiftly reduced (*6*). The resulting "cherry" consists of a platinum core and a copper mantle. When the temperature increases, the particles reconstruct to acquire some Pt atoms on the cluster surface, but are still richer in Cu than the core of the clusters. The experimental data with which this model has thus far been verified are chemical in nature, i.e., chemisorption of hydrogen was used to count the Pt atoms in the surface of the bimetallic particles, and catalytic test reactions of known sensitivity to the size of the Pt ensembles in the surface were used to qualitatively estimate the average Pt ensemble sizes.

The present paper describes work in which ^{129}Xe NMR and EXAFS have been used to characterize Pt–Cu clusters in NaY. The bimetallic Pt–Cu/NaY samples were prepared by two different modes for metal loading: simultaneous ion exchange of Cu^{2+} and $Pt(NH_3)_4^{2+}$ into NaY zeolite and sequential Cu^{2+} ion exchange into reduced Pt/NaY in which Pt clusters are already formed. ^{129}Xe NMR spectroscopy of the xenon adsorbed on highly porous supported catalysts has been found to be very useful to probe the surface structure of the catalysts. It was originally introduced by Fraissard *et al.* (*7–13*), who showed that ^{129}Xe NMR is able to probe for characteristic parameters of zeolite catalysts including void volume, acidity, cations, metal particles, and hydrogen chemisorption on these and coke deposits. In view of its large size, the Xe atom specifically probes for material inside wide channels and large cavities, whereas species inside small cavities (e.g., sodalite cages or hexagonal prisms of faujasites) are disregarded. Extended X-ray absorption fine structure is the most common physical method for determining the coordination number of the supported metal and thus for obtaining information about the particle size (*14–16*). EXAFS can usually provide information of the bulk composition.

No previous work is known to us using ^{129}Xe NMR for probing the surface structure of bimetallic clusters in zeolite cages. It appears challenging to explore the potential of this method for catalysts of this type. Nieuwenhuys *et al.* (*17–19*) have studied the nature of the adsorption bond between xenon and metal surfaces. They found a linear correlation between the change in work function due to adsorbed xenon and the isosteric heat of adsorption, which was measured in the field electron microscope. It follows from their results that the heat of adsorption and the polarization of adsorbed xenon is markedly different on platinum and copper; it therefore appears reasonable to expect that ^{129}Xe NMR might be able to distinguish between bimetallic clusters that display, e.g., a platinum-rich or a copper-rich surface. It will be very effective to characterize the supported bimetallic catalysts if the two techniques, i.e., EXAFS (a bulk-analysis technique) and ^{129}Xe NMR (a surface-analysis technique), can be used at the same time. In this work, we thus try to probe bimetallic cluster formation in Pt–Cu/NaY by EXAFS and ^{129}Xe NMR.

EXPERIMENTAL

Sample Preparation

Monometallic Pt_x/NaY samples were prepared according to a known scheme that consists of ion exchange of $Pt(NH_3)_4^{2+}$ into NaY zeolite, activation in flowing O_2, and subsequent reduction in flowing H_2. Here the subscript x following Pt denotes the number of atoms per unit cell of zeolite. The ion exchange was carried out over 12 h by magnetically stirring a high-purity NaY zeolite (prepared here by the Breck procedure (*20*)) in an aqueous solution of $Pt(NH_3)_4\,Cl_2$ at room temperature. The zeolite sample was then filtered, washed with hot doubly distilled water, and dried in vacuum oven at 330 K. The sample was placed into a Pyrex U-tube flow reactor that was jointed with an NMR tube equipped with a vertical ground-glass vacuum stopcock. The activation was then performed by flowing O_2 through a thin bed of sample at 1000 ml g^{-1} min^{-1} while

heating to 573 K at a rate of 0.5 K min^{-1}. The sample was further kept at 573 K for 2 h in flowing O_2, evacuated at 1×10^{-5} Torr, and then cooled to room temperature. The reduction was performed by flowing H_2 at 200 ml g^{-1} min^{-1} under linear heating to 573 K over 2 h and further for 2 h at 573 K. Cu_x/NaY samples were also prepared in a similar way by performing an ion exchange with $Cu(NO_3)_2$.

Two different procedures were employed in the preparation of bimetallic PtCu/NaY samples with various Cu/Pt ratios as follows: in the first procedure, Pt_x/NaY was first prepared as described above, open to air, and the sample was subsequently ion exchanged with Cu^{2+} in an aqueous solution. This sample was filtered, washed, and activated in flowing O_2 in the same way used for the preparation of Pt_x/NaY. These bimetallic samples, which were prepared by a sequential loading method, are designated as Cu_y/Pt_x/NaY. In the second procedure, $Pt(NH_3)_4^{2+}$ and Cu^{2+} ions were simultaneously exchanged into the zeolite by using an aqueous solution containing both the ions. The activation and reduction treatments were carried out in the same way described above. These bimetallic samples, prepared by a simultaneous ion exchange method, are designated as Pt_x-Cu_y/NaY. The metal loadings (x and y) were determined from the difference of the metal content in the supernatant solutions prior to and after the ion exchange analyzed by atomic absorption spectroscopy. All the samples were evacuated for 2 h at 673 K under vacuum of 1×10^{-5} Torr and then cooled to room temperature prior to further experiments *in situ* or open to air.

^{129}Xe NMR

All the calcination and reduction treatments were performed *in situ* in a flow reactor that was jointed with a specially designed NMR tube equipped with a homemade ground-glass vacuum stopcock. The sample was transferred into the NMR tube *in situ* after the preparation. The NMR tube was then sealed off by a flame under vacuum. Various pressures of xenon gas (Matheson, 99.995%) were equilibrated with the sample at 296 K for 0.5 h. ^{129}Xe NMR spectra were obtained at 296 K with a Bruker AM 300 instrument operating at 83.0 MHz for ^{129}Xe with 0.5-s relaxation delay. The chemical shift is referenced with respect to the NMR signal of the xenon in the bulk gas phase extrapolated to zero pressure.

Xenon and Hydrogen Adsorption

Two xenon adsorption isotherms were obtained volumetrically from each sample. The first isotherm was from "freshly prepared" Pt/NaY or Pt–Cu/NaY. Dioxygen (or dihydrogen) at approximately 1 atm was equilibrated with the sample. Dioxygen in the gas phase and the weakly adsorbed hydrogen were subsequently removed by evacuating for 30 min at room temperature. Then, the second isotherm was obtained.

Measurement of hydrogen chemisorption at 296 K was carried out volumetrically after all the preadsorbed hydrogen atoms were desorbed at 673 K and 1×10^{-5} Torr for 1 h and cooled at 296 K. Then hydrogen adsorption isotherm was obtained in the pressure range of 50–300 Torr at 296 K. Extrapolation of this adsorption isotherm to zero pressure gives total hydrogen chemisorption value. The sample was then evacuated at 296 K and 1×10^{-5} Torr for 1 h, and a second adsorption isotherm was measured. The difference between the two adsorption measurements, extrapolated to zero pressure, represents the irreversible chemisorption of hydrogen.

EXAFS

About 0.12 g of the sample was transformed into a disc of 10 mm in diameter in a press. The sample was rereduced in flowing H_2 at 673 K for 2 h in a flow reactor that was jointed with a cell having Kapton (Eastman Kodak) windows. After the catalyst was cooled to room temperature and transferred into the cell, the cell was sealed off by a flame under a H_2 atmosphere. The

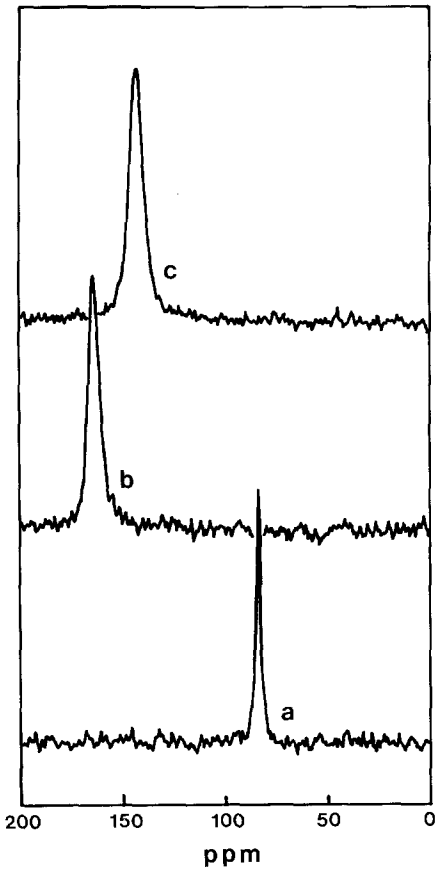

FIG. 1. ^{129}Xe NMR spectra of adsorbed xenon from (a) NaY, (b) $Pt_{7.1}/NaY$, and (c) $Cu_{7.1}/Pt_{7.1}/NaY$ show single Lorentzian peaks with various chemical shifts at 400 Torr and 296 K.

EXAFS experiments were performed by using beam line 7C at the Photon Factory of the National Laboratory for High Energy Physics (KEK-PF) in Tsukuba, Japan. The X-ray absorption measurements were carried out at the Pt L_{III} edge and Cu K edge. The data were analyzed using Pt and Cu foils as references.

RESULTS AND DISCUSSION

Figure 1 shows ^{129}Xe NMR spectra obtained from $Pt_{7.1}/NaY$, $Cu_{7.1}/Pt_{7.1}/NaY$ (which has been prepared by a sequential loading scheme), and NaY samples. All the NMR spectra show single-Lorentzian peaks with various chemical shifts in a broad range. The chemical shift comes from the physical interaction of the adsorbed xenon with other species through collisions or van der Waals complex formation. As a result, there appear marked differences in the chemical shift of xenon. Thus, the ^{129}Xe chemical shift of adsorbed xenon is very sensitive to the physicochemical environment of the zeolite cage and therefore can serve as a useful probe for studying cluster formation and growth in zeolite (*7, 13, 21–25*). The samples of zeolite-supported metals are microscopically heterogeneous as the electron micrograph in Fig. 2 shows. However, a rapid exchange of xenon between supercages and even between adjacent zeolite crystals averages the chemical shift to give a single NMR line. Such a rapid xenon exchange was qualitatively explained in previous studies (*7, 23, 25–27*). A quantitative explanation for chemical shift averaging is given below for the $Pt_{7.1}/NaY$ and $Cu_{7.1}/Pt_{7.1}/NaY$ samples.

Figure 3 shows xenon adsorption isotherms obtained from the $Pt_{7.1}/NaY$ and $Cu_{7.1}/Pt_{7.1}/NaY$ samples at 296 K. The adsorption isotherms of fresh samples have a steep curvature at low pressures, and become progressively oblique and then finally nearly linear with the pressure increase above ca. 50 Torr. The xenon adsorption isotherms obtained from the supported metal samples with chemisorbed oxygen at room temperature are just linear without such a steep increase at low pressures. Furthermore, the two xenon adsorption isotherms, which have been obtained respectively from fresh sample and with chemisorbed oxygen, have the same slopes in the high pressure linear region above 50 Torr. Recently, such phenomena in the xenon adsorption have been found to occur with various samples of other group VIII metals such as Pd, Ru, Rh, and Ir (*28*). The xenon adsorption can be rationalized as a sum of two Langmuir adsorption isotherms: one for weak adsorption on the zeolite wall and the other for strong adsorption on the

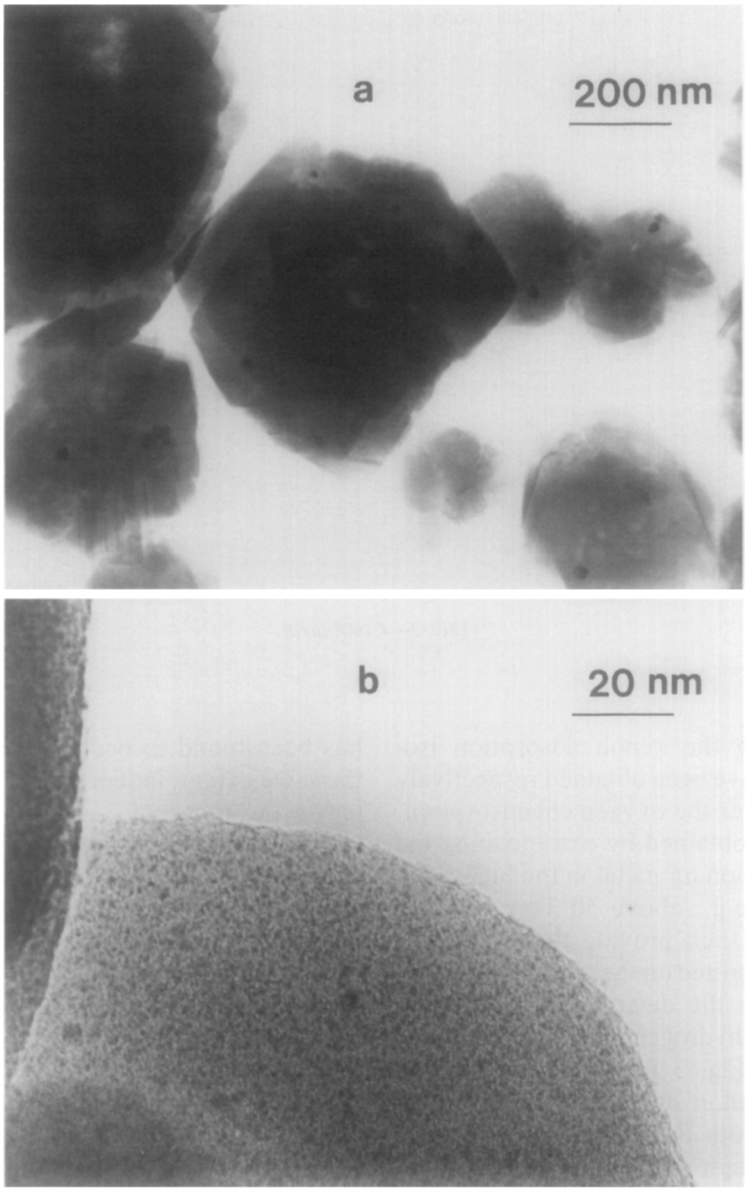

FIG. 2. Transmission electron micrographs from (a) $Cu_{2.1}$/NaY, which shows large agglomerates on the surface of zeolite, whereas those from (b) $Pt_{7.1}$/NaY and (c) $Cu_{7.1}/Pt_{7.1}$/NaY show mostly small cluster in zeolite crystal.

metal cluster. Oxygen, chemisorbed on the metal surface, inhibits xenon adsorption. Similar results can be obtained with chemisorbed hydrogen, but in the case of $Cu_{7.1}/Pt_{7.1}$/NaY hydrogen has been found to be somewhat less effective for the inhibition of the xenon–cluster interaction. The amount of xenon adsorbed on the zeolite support can be given from the xenon adsorption isotherm that has been obtained after the oxygen chemisorption, and the amount of xenon on the metal cluster is given from a differ-

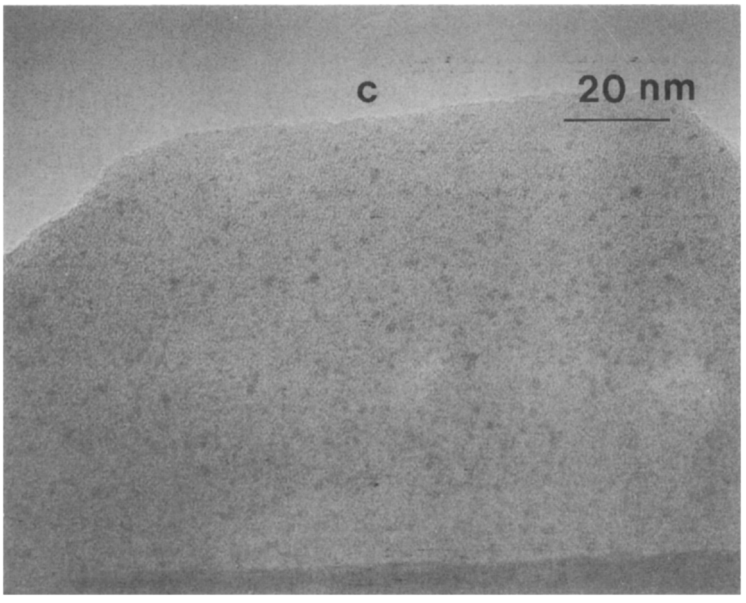

FIG. 2—*Continued*

ence between the xenon adsorption isotherms that have been obtained respectively before and after the oxygen chemisorption. An intercept obtained by extrapolating the amount of xenon on metal in the high-pressure region, e.g., above 50 Torr, to zero pressure will then provide the amount of xenon gas saturated on the clusters in a manner similar to the determination of metal dispersion by hydrogen chemisorption (*29*). The data in Fig. 3 give nearly the same amount of xenon adsorbed on the metal clusters for both the $Pt_{7.1}$/NaY and $Cu_{7.1}$/$Pt_{7.1}$/NaY samples. The cluster size concerning these data is discussed below. Recently, such a method using xenon adsorption has been applied to the study of the size of various group VIII metals supported on faujasite-type zeolite (*28, 30*). The slope in the high-pressure region in Fig. 3 decreases considerably after Cu loading. That is, the amount of xenon adsorbed on the support can decrease after Cu loading. Similarly, Pt loading on NaY results in a decrease of the amount of xenon adsorption on the support. The slope decrease in the xenon adsorption has been found to occur approximately to the same extent, independent of the Pt loading in the range of 2–10 wt% Pt on NaY (*30*), and thus it may come from a structural change of the zeolite due to the metal loading treatments, e.g., calcination.

Since xenon exchanges very rapidly between the supported Pt cluster and the zeolite wall, the chemical shift δ in ^{129}Xe NMR of the adsorbed xenon gas can approximately be written as

$$\delta = (n_{Pt}\delta_{Pt} + n_{sup}\delta_{sup})/(n_{Pt} + n_{sup}), \quad (1)$$

where n_{Pt} and δ_{Pt} denote the amount and the chemical shift of xenon adsorbed on the cluster and n_{sup} and δ_{sup} are those on the support, respectively. Approximately, δ_{sup} is the same as the chemical shift of xenon adsorbed on the NaY zeolite under the same concentration of the adsorbed xenon. With a value of δ_{Pt} = 1300 ppm, a very good fit has been obtained for the experimental values as shown in Fig. 4. According to the above interpretation for the xenon adsorption isotherm, n_{sup} becomes much greater than n_{Pt} at sufficiently high pressures, e.g.,

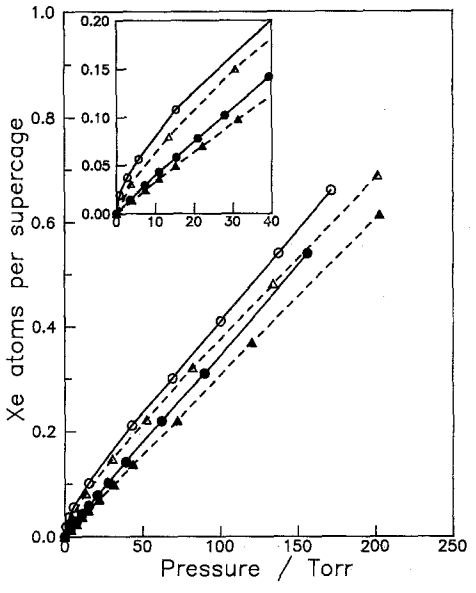

FIG. 3. Xenon adsorption isotherms obtained at 296 K from $Pt_{7.1}$/NaY (○) and $Cu_{7.1}/Pt_{7.1}$/NaY (△) can be interpreted with strong adsorption of xenon on the metal cluster and weak adsorption on the zeolite wall. However, xenon adsorption isotherms from $Pt_{7.1}$/NaY (●) and $Cu_{7.1}/Pt_{7.1}$/NaY (▲) after oxygen chemisorption display only the weak xenon adsorption on the support. High-pressure extrapolation of adsorption isotherms to zero pressure gives 0.061, 0.005, 0.066, and 0.003 for $Pt_{7.1}$/NaY and $Cu_{7.1}/Pt_{7.1}$/NaY before and after oxygen chemisorption, respectively.

above 200 Torr. Then, the chemical shift in Eq. (1) becomes approximately proportional to n_{Pt} for the same zeolite support, and therefore the chemical shift δ increases linearly with the metal loading. In the case of our sequential Pt–Cu loading on NaY zeolite, the second metal (i.e., Cu) may form a bimetallic Pt–Cu cluster by combining with the Pt cluster, or it may form a separate cluster in a vacant supercage or on the external surface of the zeolite. If Cu forms a separate cluster (i.e., monometallic cluster) during the Cu loading on $Pt_{7.1}$/NaY, the equation for δ will approximately become

$$\delta = \delta_{Pt}n_{Pt}/n + \delta_{Cu}n_{Cu}/n + \delta_{sup}n_{sup}/n, \quad (2)$$

where n is $n_{Pt} + n_{Cu} + n_{sup}$. Since n_{sup} can be assumed to be much greater than n_{Pt} or n_{Cu} at sufficiently high pressures, the chemical shift can be increased approximately by $\delta_{Cu}n_{Cu}/n$ from Eq. (1) to Eq. (2). In case Cu forms large agglomerates on the external surface of the zeolite, the total surface area of Cu interacting with xenon will be very small and therefore n_{Cu} will be negligible compared to n_{Pt}. Then, the second term in Eq. (2) coming from a contribution by Cu clusters will be neglected, and thus there will be no increase in δ by Cu. If small Cu clusters are formed in vacant supercages, n_{Cu} may be comparable to n_{Pt}, and the chemical shift increase by $\delta_{Cu}n_{Cu}/n$ will be significant. The chemical shift should thus be increased further or at least should not be decreased if monometallic Cu cluster is formed by Cu loading on $Pt_{7.1}$/NaY. There is also no evidence, under the present experimental conditions, that the Pt clusters migrate onto the external surface of zeolite crystals during the Cu loading, resulting in a decrease of the chemical shift. Therefore,

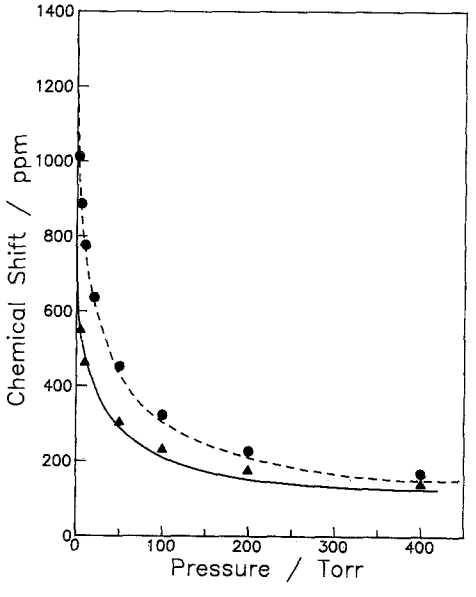

FIG. 4. Chemical shift in ^{129}Xe NMR of adsorbed xenon at 296 K is plotted as a function of pressure. ●, $Pt_{7.1}$/NaY-experimental; --, $Pt_{7.1}$/NaY-calculated with δ_{Pt} = 1300 ppm by Eq. (1); ▲, $Cu_{7.1}/Pt_{7.1}$/NaY-experimental; —, $Cu_{7.1}/Pt_{7.1}$/NaY-calculated with δ_{Pt-Cu} = 800 ppm.

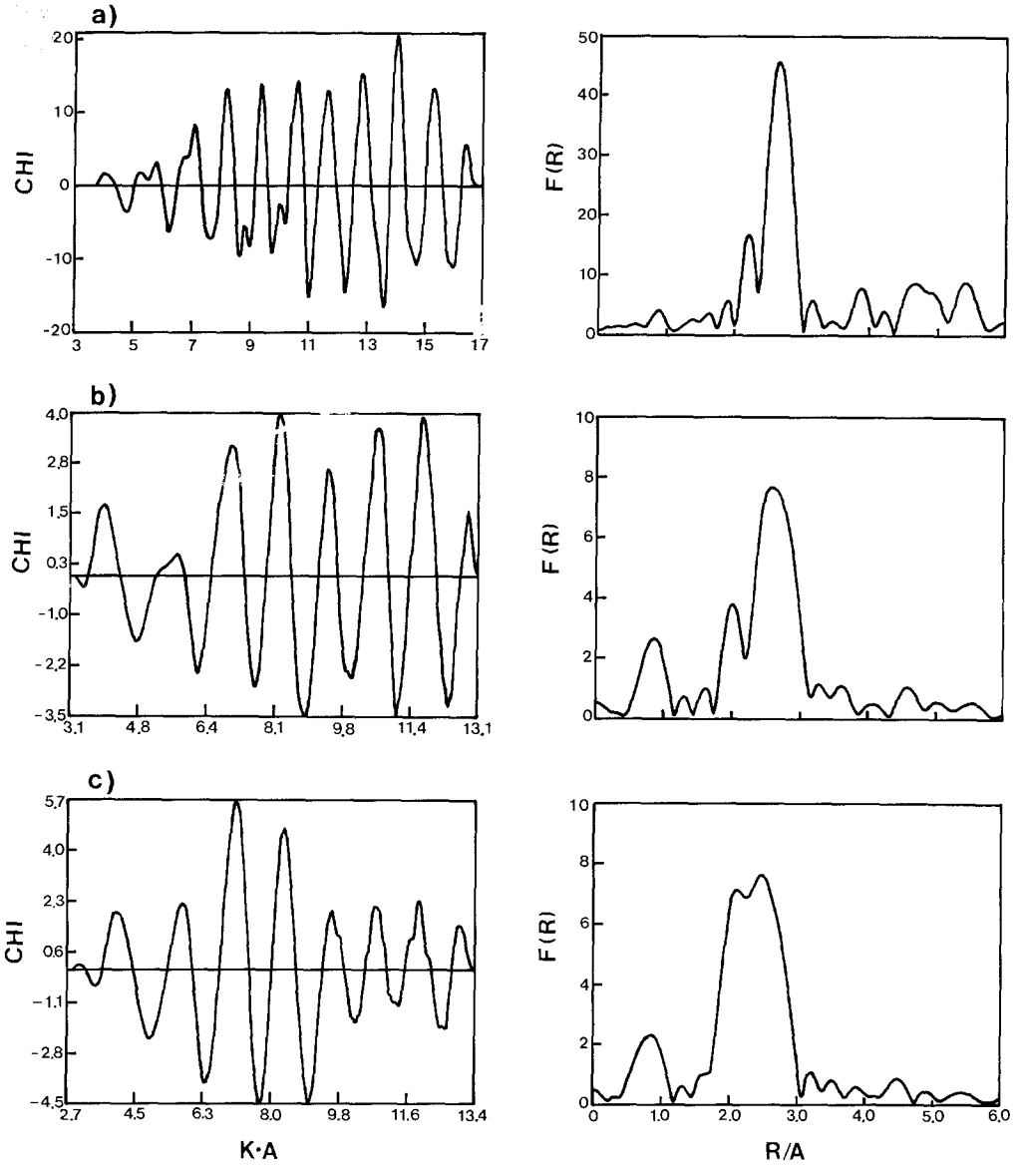

FIG. 5. Fourier transforms of EXAFS spectra at Pt L_{III} for (a) Pt foil, (b) $Pt_{7.1}$/NaY, and (c) $Cu_{7.1}$/$Pt_{7.1}$/NaY.

the chemical shift decrease from $Pt_{7.1}$/NaY to $Cu_{7.1}$/$Pt_{7.1}$/NaY under the same experimental conditions, as shown in Fig. 4, can indicate that bimetallic Pt–Cu clusters are formed in the zeolite cages. By substituting Pt–Cu for Pt in Eq. (1) and using δ_{Pt-Cu} = 800 ppm, a good fit has also been obtained for the $Cu_{7.1}$/$Pt_{7.1}$/NaY sample as shown in Fig. 4. The parameters δ_{Pt} and δ_{Pt-Cu} can be regarded as chemical shift of xenon adsorbed on the metal cluster, which is independent of the metal content. The decrease from 1300 to 800 ppm can confirm that the interaction of xenon with the metal cluster changes probably due to the formation of bimetallic Pt–Cu cluster upon variation

from $Pt_{7.1}$/NaY to $Cu_{7.1}/Pt_{7.1}$/NaY. In this way, the magnitude of δ_M (where M denotes "metal") may be used as a good parameter in the study of other bimetallic clusters supported on zeolites.

Fourier transforms of EXAFS spectra for $Pt_{7.1}$/NaY and $Cu_{7.1}/Pt_{7.1}$/NaY are shown in Fig. 5. In the case of $Pt_{7.1}$/NaY, there appears a peak at Pt–Pt coordination distance (i.e., 0.277 nm). Another small peak at about 0.22 nm is caused by nonlinearity of the phase shift function for Pt–Pt bonding (*31*). For $Cu_{7.1}/Pt_{7.1}$/NaY, there appears another peak probably due to Pt–Cu coordination. If the Pt and Cu atoms form a uniform alloy cluster, the intensity at Pt–Pt distance should decrease significantly after loading Cu subsequently. Although it has not been attempted to obtain the coordination number by the curve-fitting method, it appears that the intensities at Pt–Pt distance in the Fourier transforms are very similar for both samples. Thus, there seems to exist no appreciable difference in the Pt–Pt coordination structure. It may be concluded from the above results from ^{129}Xe NMR and EXAFS that a bimetallic Pt–Cu cluster is formed by the adsorption of Cu on the Pt cluster during the reduction of the Cu precursor, and the Cu atoms remain in the outer rim of the resulting bimetallic cluster according to a model of "Pt cluster covered by Cu atoms." If the metal cluster grows very much into adjacent supercages by the Cu adsorption onto the Pt cluster, the high-pressure extrapolated intercept from the xenon adsorption isotherms shown in Fig. 3 will increase considerably. In fact, the intercept has been found to increase only a little by Cu loading on $Pt_{7.1}$/NaY: 0.061 ± 0.005 for $Pt_{7.1}$/NaY and 0.066 ± 0.005 for $Cu_{7.1}/Pt_{7.1}$/NaY in terms of xenon atoms per supercage, respectively. This suggests that the cluster size of the bimetallic PtCu does not exceed the supercage size significantly.

To investigate whether similar bimetallic Pt–Cu clusters can be obtained in the case of simultaneous Pt–Cu loading on NaY zeolite, a series of $Pt_{2.1}$–Cu_x/NaY with various x have been studied by ^{129}Xe NMR spectroscopy. The results in Fig. 6 show decreases in the chemical shift from $Pt_{2.1}$/NaY to $Pt_{2.1}$–$Cu_{2.1}$/NaY under given pressures, which is similar to the above results obtained with $Pt_{7.1}$/NaY and $Cu_{7.1}/Pt_{7.1}$/NaY. Thus, the reduction of the Cu-precursor species has resulted in the formation of bimetallic Pt–Cu clusters regardless of the two different modes for metal loading. On the other hand, reduction of Cu^{2+} without Pt results in the formation of large agglomerates on the external surface of zeolites as a transmission electron micrograph in Fig. 2 shows. In such a case of Cu/NaY, the chemical shift of xenon becomes almost the same as that of pure NaY as Fig. 6 shows. This agrees with previous results obtained by using temperature-programmed reduction (*6*).

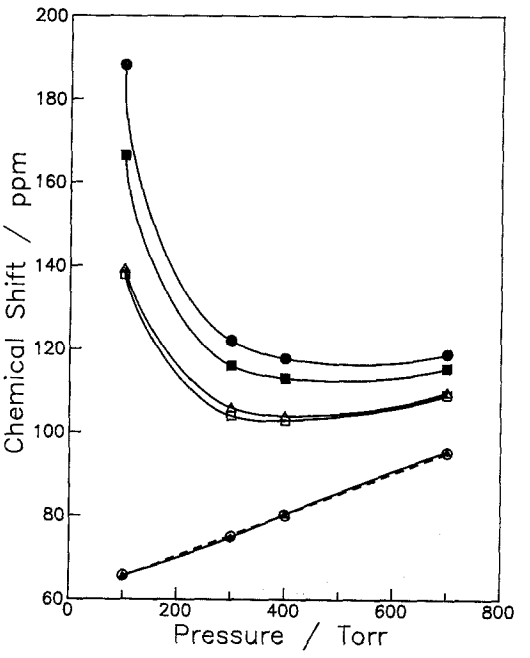

FIG. 6. Chemical shift in ^{129}Xe NMR of adsorbed xenon at 296 K is plotted as a function of pressure. ●, $Pt_{2.1}$/NaY; ■, $Pt_{2.1}$–$Cu_{0.8}$/NaY; □, $Pt_{2.1}$–$Cu_{1.6}$/NaY; △, $Pt_{2.1}$–$Cu_{2.1}$/NaY; -▲-, $Cu_{2.1}$/NaY; --○--, NaY.

Table 1 lists the results of hydrogen chemisorption and ^{129}Xe NMR for the Pt/NaY

TABLE 1

H/Pt Values by Hydrogen Chemisorption, the Chemical Shift (δ) at 296 K under 400 Torr Xenon, and the Chemical Shift of Xenon Adsorbed on the Cluster (δ_{metal}) in ^{129}Xe NMR

Sample	$(H/Pt)_{total}$	$(H/Pt)_{irrev.}$	δ	δ_{metal}
$Pt_{7.1}$/NaY	1.28	0.82	169	1300
$Cu_{7.1}/Pt_{7.1}$/NaY	0.74	0.44	144	800
$Pt_{2.1}$/NaY	1.37	0.93	115	—
$Pt_{2.1}$–$Cu_{0.8}$/NaY	1.10	0.65	108	—
$Pt_{2.1}$–$Cu_{1.6}$/NaY	1.04	0.60	106	—
$Pt_{2.1}$–$Cu_{2.1}$/NaY	1.06	0.61	107	—
$Cu_{2.1}$/NaY	0.00	0.00	85	—

and Pt–Cu/NaY samples. The hydrogen chemisorption on the metal cluster decreases due to the Cu loading. The overall surface composition may be determined from irreversible hydrogen chemisorption data according to a previous result by Moretti and Sachtler (*6*); $(H/Pt)_{Pt-Cu/NaY}/(H/Pt)_{Pt/NaY}$ is the Pt dispersion assuming that Cu does not chemisorb hydrogen. From the data in Table 1, $(H/Pt)_{Pt-Cu/NaY}/(H/Pt)_{Pt/NaY}$ is approximately equal to $(\delta_{Pt-Cu}-\delta_{NaY})/(\delta_{Pt}-\delta_{NaY})$, where δ_{NaY} is the chemical shift of xenon adsorbed on NaY extrapolated to zero pressure (i.e., 60 ppm). It thus appears that the chemical shift decrease by the Cu loading is proportional to the Cu coverage on the cluster surface. However, care should be taken to extrapolate such a result to other systems. It may be possible to use the ^{129}Xe NMR technique to determine the overall surface composition for a simple case in which the metal surface consists of fairly large separate Cu and Pt domains so that Eq. (2) can be applied. On the other hand, it would be difficult to assume this relation for other small bimetallic clusters located in zeolite supercages, which have a substantial electronic effect due to bimetallic clustering. Similarly, Boudart *et al.* (*32*) reported that the decrease in the chemical shift of xenon on Pt/NaY is not proportional to the concentration of the chemisorbed hydrogen.

CONCLUSION

This study has shown that ^{129}Xe NMR of the adsorbed xenon is useful for the study of bimetallic Pt–Cu clusters supported on Y zeolites. Further, combination of the ^{129}Xe NMR technique (a surface analysis technique) and EXAFS (a bulk analysis technique) is more effective for the characterization of the supported bimetallic Pt–Cu cluster than the application of either single technique. A combination of these methods will be powerful for the characterization of other zeolite-supported bimetallic catalysts.

ACKNOWLEDGMENTS

R. Ryoo acknowledges support from the Korea Science and Engineering Foundation and from the Synchrotron Radiation User Training Program of the Pohang Light Source for travel for EXAFS experiments. W. M. H. Sachtler gratefully acknowledges support from the U.S. Department of Energy, Grant DE-FGO2-87ERA3654. The authors express gratitude to Professor Jeong Yong Lee of the Korea Advanced Institute of Science and Technology for transmission electron micrographs.

REFERENCES

1. Augustine, S. M., and Sachtler, W. M. H., *J. Catal.* **106,** 417 (1987).
2. Augustine, S. M., and Sachtler, W. M. H., *J. Phys. Chem.* **91,** 5935 (1987).
3. Augustine, S. M., Nacheff, M. S., Tsang, C. M., Butt, J. B., and Sachtler, W. M. H., *in* "Studies Surface Science and Catalysis, Vol. 38: Catalysis 1987, Proceedings, 10th North American Meeting of the Catalysis Society, San Diego, CA, May 17–22, 1987" (J. W. Ward, Ed.), p. 1. Elsevier, Amsterdam, 1988.
4. Augustine, S. M., Nacheff, M. S., Tsang, C. M., Butt, J. B., and Sachtler, W. M. H., *in* "Proceedings, 9th International Congress on Catalysis, Calgary, 1988" (M. J. Phillips and M. Ternan, Eds.), Vol. 3, p. 1190. Chem. Institute of Canada, Ottawa, 1988.
5. Augustine, S. M., and Sachtler, W. M. H., *J. Catal.* **116,** 184 (1989).
6. Moretti, G., and Sachtler, W. M. H., *J. Catal.* **115,** 205 (1989).
7. de Menorval, L.-C., Fraissard, J. P., and Ito, T., *J. Chem. Faraday Trans. 1* **78,** 403 (1982).
8. Ito, T., and Fraissard, J. P., *J. Chem. Phys.* **76,** 5225 (1982).
9. Fraissard, J. P., Ito, T., de Menorval, L.-C., and Springuel-Huet, M. A. *in* "Studies in Surface Science and Catalysis, Vol. 12: Proceedings, Work-

shop on Metal Microstructure in Zeolites, Bremen, September 22–24, 1982" (P. A. Jacobs, Ed.), p. 179. Elsevier, Amsterdam, 1982.
10. Fraissard, J. P., Ito, T., and de Menorval, L.-C., *in* "Proceedings, 8th International Congress on Catalysis, Berlin, 1984," Vol. III, p. 25. Dechema, Frankfurt-am-Main, 1984.
11. Demarquay, J., and Fraissard, J. P., *Chem. Phys. Lett.* **136,** 314 (1987).
12. Ito, T., Bonardet, J. L., Fraissard, J. P., Nagy, J. B., Andre, C., Gabelica, Z., and Derouane, E. G., *Appl. Catal.* **43,** L5 (1988).
13. Petrakis, L., Springuel-Huet, M. A., Ito, T., Hughes, T. R., Chan, I. Y., and Fraissard, J. P., *in* "Proceedings, 9th International Congress on Catalysis Calgary, 1988" (M. J. Phillips and M. Teman, Eds.), Vol. I, p. 348. Chem. Institute of Canada, Ottawa, 1988.
14. Kip, B. J., Duivenvoorden, F. B. M., Koningsberger, D. C., and Prins, R., *J. Catal.* **105,** 26 (1987).
15. Greegor, R. B., and Lytle, F. W., *J. Catal.* **63,** 476 (1980).
16. Bazin, D., Dexpert, H., Bournonville, J. P., and Lynch, J., *J. Catal.* **123,** 86 (1990).
17. Nieuwenhuys, B. E., and Sachtler, W. M. H., *Surf. Sci.* **45,** 513 (1974).
18. Nieuwenhuys, B. E., Meijer, D. Th., and Sachtler, W. M. H., *Phys. Status Solidi A* **24,** 115 (1974).
19. Nieuwenhuys, B. E., and Sachtler, W. M. H., *J. Colloid Interface Sci.* **58,** 65 (1976).
20. Breck, D. W., "Zeolite Molecular Sieves—Structure, Chemistry, and Use." Wiley, New York, 1974.
21. Chmelka, B. F., Ryoo, R., Liu, S. B. de Menorval, L.-C., Radke, C. J., Petersen, E. E., and Pines, A., *J. Am. Chem. Soc.* **110,** 4465 (1988).
22. Chmelka, B. F., de Menorval, L.-C., Csencsits, R., Ryoo, R., Liu, S. B., Radke, C. J., Petersen, E. E., and Pines, A., *in* "Studies in Surface Science and Catalysis, Vol. 48: Structure and Reactivity of Surfaces" (C. Morterra, A. Zecchina, and G. Costa, Eds.), p. 269. Elsevier, Amsterdam, 1989.
23. Shoemaker, R., and Apple, T. *J. Phys. Chem.* **91,** 4024 (1987).
24. Scharpf, E. W., Crecely, R. W., Gates, B. C., and Dybowski, C., *J. Phys. Chem.,* **90,** 9 (1986).
25. Yang, O. B., Woo, S. I., and Ryoo, R., *J. Catal.* **123,** 375 (1990).
26. Ryoo, R., Pak, C., and Chmelka, B. F., *Zeolites* **10,** 790 (1990).
27. Ryoo, R., Pak, C., Ahn, D. H., de Menorval, L.-C., and Figueras, F., *Catal. Lett.* **7,** 417 (1990).
28. Kim, J.-G., Ihm, S.-K., Lee, J. Y., and Ryoo, R., *J. Phys. Chem.,* **95,** in press (1991).
29. Benson, J., and Boudart, M., *J. Catal.* **4,** 704 (1965).
30. Ryoo, R., *in* "Catalytic Science and Technology, Vol. 1: Proceedings, 1st Tokyo Conference on Advanced Catalytic Science and Technology, July 1–5, 1991" (S. Yoshida, N. Takezawa, and T. Ono, Eds.), p. 405. Kodansha, 1991.
31. Teo, B. K., and Lee, P. A., *J. Am. Chem. Soc.* **101,** 2815 (1979).
32. Boudart, M., Samant, M. G., and Ryoo, R., *Ultramicroscopy* **20,** 125 (1986).